ELSEVIER

Thermochimica Acta 280/281 (1996) 127–151

thermochimica acta

Non-steady-state effects in the kinetics of crystallization of organic polymer glass-forming melts[1]

A. Dobreva[a,*], A. Stoyanov[b], S. Tzuparska[b], I. Gutzow[a]

[a] *Institute of Physical Chemistry, Bulgarian Academy of Sciences, Sofia 1113, Bulgaria*
[b] *Institute of Kinetics and Catalysis, Bulgarian Academy of Sciences, Sofia 1113, Bulgaria*

Abstract

A critical analysis of different theoretical models of overall crystallization kinetics accounting for non-steady-state nucleation effects as well as for size-dependent cluster growth is given. The overall crystallization kinetics of polyethylene terephthalate (unfilled and also containing titanium dioxide) is studied near the melting temperature T_m, and in the vicinity of the glass transition temperature T_g, under conditions of sporadic and athermal nucleation, respectively, by using differential scanning calorimetry (DSC) and optical microscopy. A standard method is proposed for analyzing the degree of transformation vs. time curves in order to determine the kinetic parameters of the process from DSC measurements. The temperature dependence of the induction times τ_{ind} shows that, in the vicinity of the glass transition temperature, they are determined by non-steady-state nucleation kinetics. In this way, it is shown that the more general, transient formulation of the classical theory of phase formation is also inherent to polymer crystallization kinetics.

Keywords: Crystallization; Kinetics; Melt; Polymer

1. Introduction and historical background

The theoretical analysis performed by Zeldovich [1] (see also Refs. [2–5]) shows that by its very physical nature the nucleation process is of a non-steady-state character. This theoretical prediction has been confirmed by computer simulation [6] as well as

* Corresponding author.
[1] Dedicated to Professor Hiroshi Suga.

SSDI 0040-6031(95)02639-8

by experimental evidence [7–9]. The basic parameter in the kinetics of transient nucleation, the non-steady-state time lag τ, is proportional to the viscosity of the ambient phase. Taking into account the high viscosity of glass-forming liquids, it has to be expected, as already pointed out by several authors [10–12], that non-steady-state effects in glass-forming systems should be of measurable duration. Thus, time lags up to several hours have to be anticipated in the vicinity of the glass transition temperature. Experimental evidence for the significance of non-steady-state effects in the nucleation of inorganic glass-forming systems, beginning with the first experimental proof given by Gutzow et al. [7] for the case of sodium metaphosphate, has been analyzed and reconsidered in a number of survey articles [12, 13].

Experimental results obtained with metal glass-forming alloys [14] also reveal the transient character of nucleation in these systems.

Non-steady-state effects should also be observed in the crystallization of organic polymer glass-forming liquids as there is no structural or other reason why the transient character of the nucleation process should be excluded in these systems. On the contrary, accounting for the particular structure of organic polymers and the possibility of macromolecular entanglements, it is to be expected that non-steady-state effects should be of even greater importance in polymers than in the already cited cases. However, one of the first analyses of the nucleation kinetics in polymer liquids, performed by Flory and McIntyre [15] for polydecamethylene cebacate, indicates that the induction times observed in this polymer in the vicinity of the melting temperature T_m are reciprocal to the steady-state nucleation rate in the considered temperature interval, i.e. in this case non-steady-state effects are insignificant. The same conclusion can also be drawn from our analysis [16] of the number of nuclei vs. time curves for polydecamethylene terephthalate reported by Sharples and Swinton [17, 18].

In the present contribution, the possibility of proving non-steady-state effects in the nucleation of organic chain-folding polymers is re-examined. The main efforts are concentrated at high undercoolings in the vicinity of the glass transition temperature T_g, where the transient character of the nucleation process should be most pronounced. Polyethylene terephthalate (PET) is chosen as a model system.

From an experimental point of view, PET is a very convenient model, having a relatively low melting temperature T_m (about 542 K), and a sufficiently high glass transition temperature T_g (about 342 K). The latter means that it can be quenched from the molten state to give a completely amorphous material at room temperature. The vitrified polymer does not crystallize at room temperatures, thus allowing convenient examination of the quenched samples. In addition, PET has been the subject of many experimental studies so that the most significant molecular constants of this polymer are known. A thorough thermodynamic and rheological investigation of PET has also been performed [16]. Moreover PET is one of the few polymers for which the temperature dependence of the rate of crystal growth has been examined over the whole range of crystallization temperatures [19, 20]. Furthermore, secondary crystallization effects in the overall crystallization kinetics in PET are negligible, which additionally simplifies the analysis.

It has to be mentioned, however, that in the low temperature region in the vicinity of the glass transition temperature T_g, where non-steady-state effects are of particular

significance, the nucleation rate of undercooled organic polymer glass-forming systems, as a rule, is very high and the determination of the number of grown nuclei vs. time dependences, usually employed in this type of investigations (see Ref. [12]), is associated with considerable experimental difficulties. This is why we have chosen another approach for studying the possible significance of non-steady-state effects in organic polymer glass-forming systems: analysis of the overall crystallization kinetics.

The kinetics of the isothermal overall crystallization process in organic polymers and especially in PET has been thoroughly investigated by a number of authors [21–24]; and various methods have been employed to determine the degree of transformation vs. time $\alpha(t)$ curves. However, to our knowledge, no attempt has been made so far to analyze $\alpha(t)$ curves for organic polymers from the standpoint of the more general, non-steady-state formulation of the present day nucleation theory. An account of the first derivation of this general formalism can be found in Refs. [25] and [26].

In the present investigation, the kinetics of isothermal overall crystallization is examined by differential scanning calorimetry (DSC) and hot-stage optical microscopy. Two types of experiments were performed: crystallization with sporadic nucleation and crystallization taking place in the presence of athermal nuclei. Crystallization both from the molten state (in the vicinity of T_m) and from the glassy state (devitrification above T_g) was studied. The influence of a nucleation-active filler (TiO_2) was also examined. In performing the analysis of the experimental results, data previously obtained in our laboratory on the rheology and thermodynamics of the same PET samples were used [16].

2. Kinetics of overall crystallization: basic formalism

The classical description of the overall crystallization kinetics has been given independently by Kolmogorov [27], Johnson and Mehl [28] and Avrami [29]. In the derivation made by Kolmogorov, the formalism of the theory of probability and a model stemming, in fact, from a problem already discussed by Poisson were used. Avrami performed a geometric treatment and introduced the concept of the so-called extended volume, $Y_n(t)$. The theorem connecting the extended volume $Y_n(t)$ with the degree of transformation α reads

$$d\alpha = (1-\alpha)d[Y_n(t)] \tag{1a}$$

or, after integration

$$\alpha = 1 - \exp[-Y_n(t)] \tag{1b}$$

where $Y_n(t)$ is connected with nucleation rate $I(t)$ and the growth rate $G(t)$, as

$$Y_n(t) = \bar{\omega}' \int_0^t I(t) G^{n'}(t)(t-t')^{n'} dt' \tag{2a}$$

Here n' is determined by the dimensionality of growth and $\bar{\omega}'$ is a shape factor, e.g. for spherical symmetry $n' = 3$ and $\bar{\omega}' = 4\pi/3$.

Assuming that $I(t) = \text{const} = I_0$, and $G(t) = \text{const} = G_\infty$, as done by the above-mentioned authors, $Y_n(t)$ becomes

$$Y_n(t) = \bar{\omega}' I_0 G_\infty^{n'} \int_0^t (t - t')^{n'} \mathrm{d}t' \tag{2b}$$

and

$$\alpha = 1 - \exp[-\bar{\omega} I_0 G_\infty^{n-1} t^n] = 1 - \exp[-K t^n] \tag{3a}$$

Here $n = n' + 1$, $\bar{\omega} = \bar{\omega}'/n'$, and K is the overall crystallization rate coefficient. The dependence of the degree of transformation on time has a sigmoidal course for $n > 1$.

Avrami also considered the case when nucleation takes place on N^* active sites (athermal nucleation). Then Eq. (1b) becomes

$$\alpha = 1 - \exp[-\bar{\omega} N^* G_\infty^{n-1} t^{n-1}] = 1 - \exp[-K_a t^{n-1}] \tag{3b}$$

In the following, the notations K_a and K_s are used for athermal and sporadic crystallization, respectively. In the athermal case, the Avrami exponent is diminished by unity and N^* appears in K_a instead of I_0.

The kinetics of transformation, which proceeds via surface-induced growth of an ensemble of equal grains of size R, has been derived by Mampel [30] and Todes [31]. For this more complicated crystallization model, no simple analytical solution is possible but, nevertheless, it can be shown that, to a first approximation, the Mampel–Todes $\alpha(t)$ curves can also be analyzed in terms of the Avrami $\log(-\log(1-\alpha))$ vs. $\log t$ plots. In the Mample–Todes analysis, however, n loses its physical meaning given in the classical formulation.

At the end of 1960s, after the significance of the non-steady-state effects in the crystallization of glass-forming systems had been established, Gutzow and Kashchiev [25] reconsidered the overall crystallization kinetic problem assuming that $I(t)$ is a time-dependent function in the sense introduced by Zeldovich. In this first analysis accounting for the transient character of $I(t)$, the Collins–Kashchiev expression [4, 5] for the time dependence of the nucleation rate, $I(t)$, was used.

In a following quite recent development, Schneidman and Weinberg [32] showed that not only the time dependence of the nucleation rate due to non-steady-state effects but also the size dependence of the growth rate may influence the course of the $\alpha(t)$ curves under isothermal conditions. In a first approximation, the size dependence of the growth rate $G(R)$ can be written as

$$G(R) = G_\infty \left(1 - \frac{R}{R_c}\right) \tag{4}$$

R_c being the radius of the critical cluster.

An alternative way of solving the same problem was given by Shi and Seinfeld [33] who derived an expression for the rate of formation of overcritical clusters $I(g_0, t)$, which are so large that their decay rate is zero and only deterministic growth is operable (nucleated cluster size, g_0). In this way, Shi and Seinfeld gave an expression for $\alpha(t)$ including corrections for both the time-dependence of $I(t)$ and the size-dependence of $G(R)$ by introducing the nucleated cluster size g_0.

All three above-mentioned extensions of the classical theory can be given in a form originally proposed by Gutzow and Kashchiev [25], i.e.

$$\alpha = 1 - \exp[-Kt^n\psi_n(t)] \tag{5}$$

where $\psi_n(t)$ is a correction function. For $n = 4$, it has the form

$$\psi_n(t) = 1 - \frac{2\pi^2}{3}\left(\frac{\tau}{t}\right) + \frac{7\pi^4}{30}\left(\frac{\tau}{t}\right)^2 - \frac{31\pi^6}{630}\left(\frac{\tau}{t}\right)^3 + \frac{127\pi^8}{25200}\left(\frac{\tau}{t}\right)^4 + 48\left(\frac{\tau}{t}\right)^4 \sum_{m=1}^{\infty} \frac{(-1)^m}{m^8} \exp\left(-m^2\frac{t}{\tau}\right) \tag{5a}$$

for the Gutzow–Kashchiev treatment

$$\psi_n(t) = 1 - 4\left(\frac{\tau_e}{t}\right)^4 + 24\left(\frac{\tau}{t}\right)^4 \sum_{m=1}^{\infty} \frac{(-q)^m}{m^4 m!}\left[\exp\left(-m\frac{t}{\tau}\right) - 1 + m\frac{t}{\tau} - \frac{1}{2}\left(m\frac{t}{\tau}\right)^2\right] \tag{5b}$$

for the Shi–Seinfeld analysis and

$$\psi_n(t) = \left[1 - \frac{\tau}{t}\ln\left(\left(\frac{A_{k3}}{kT}\right)\left(\frac{t}{\tau}\right)\right)\right]^n \tag{5c}$$

for the Shneidman–Weinberg solution.

In above equations, τ is the non-steady-state time lag, τ_e in Eq. (5b) is an effective time lag connected with the nucleated size g_0, A_{k3} is the thermodynamic work of formation of three-dimensional nuclei, and k denotes the Boltzmann constant.

In all three solutions, the simplest possible approximation for $I(t)$, introduced first by Gutzow and Kashchiev [25] (see also Gutzow et al. [7]) in the form of a step function, can be used, i.e.

$$I(t) = \begin{cases} 0 & 0 \leqslant t \leqslant b\tau \\ I_0 & b\tau < t < \infty \end{cases} \tag{6}$$

which provides a straightforward approach to considering the influence of different factors as well as in analyzing experimental results. With this approximation, $\psi_n(t)$ also becomes a step function, which in the Gutzow–Kashchiev solution has the form

$$\psi_n(t) = \begin{cases} 0 & 0 \leqslant t \leqslant b\tau \\ (1 - b(\tau/t))^n & b\tau < t < \infty \end{cases} \tag{5d}$$

b being a numerical constant close to unity [25].

The same step function for $I(t)$ was also used by Shneidman and Weinberg [32] in deriving Eq. (5c).

The $\psi_4(t)$ correction functions and the respective $\alpha(t)$ curves are shown in Fig. 1.

In analyzing the kinetics of overall crystallization accounting for non-steady-state nucleation rate and size-dependent growth of clusters, our task is:

(i) to bring the experiment into compliance with the above-discussed solutions;
(ii) to propose a standard method for analyzing experimental data;

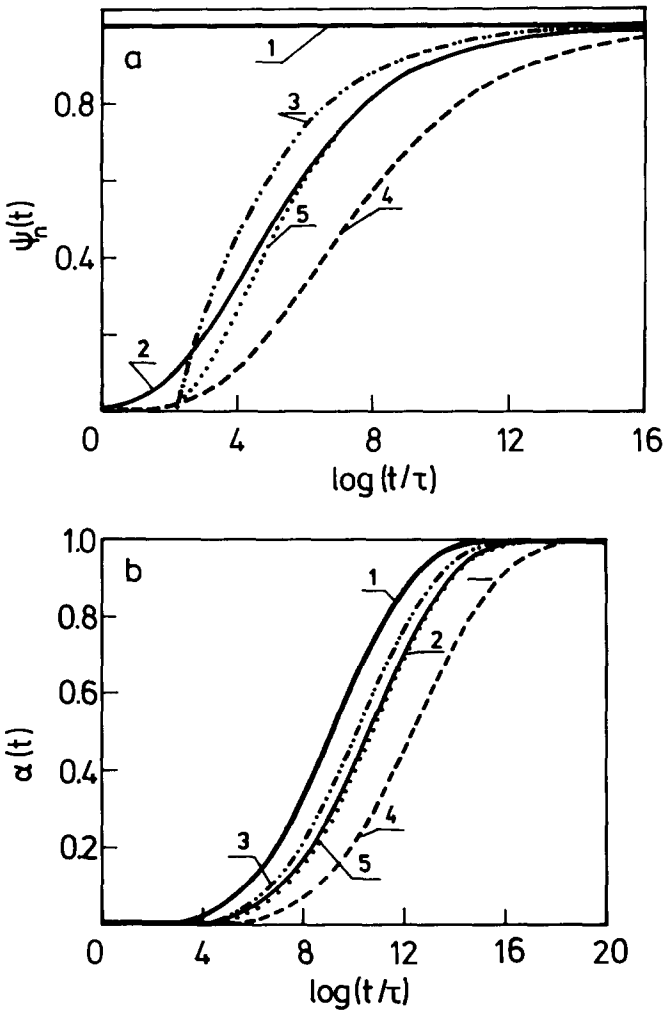

Fig. 1. Correction functions $\psi_n(t)$: (a) according to Eqs. (5), and (b) corresponding $\alpha(t)$ curves for $n = 4$: 1, classical Kolmogorov–Avrami dependence with $\psi_n(t) = 1$; 2, Gutzow–Kashchiev dependence (Eq. (5a)); 3, Shi–Seinfeld dependence (Eq. (5b)) with $\tau_e = 1$; 4, Shneidman–Weinberg dependence (Eq. (5c)) with $A_{k3}/kT = 2$; 5, approximate step-function dependence (Eq. (5d)) with $b = 1.6$. In all cases, $K = 1 \times 10^{-4}\,s^{-4}$.

(iii) to use this method for examining the results obtained for our particular experimental models.

First, however, we have to investigate under which conditions and in which temperature regions non-steady-state effects are most significant. This analysis is performed in Section 4, below. In the following section some of the necessary basic dependences of the theory of phase formation are summarized.

3. Basic dependences of the theory of nucleation and growth

The temperature dependence of the steady-state nucleation rate I_0 and the growth rate G, determining the rate coefficient K, are usually written in the form [26]

$$I_0 = N_1 D_{k3} \Gamma_3 \exp\left(-\frac{A_{k3}}{kT}\right) \tag{7}$$

and

$$G_N = \alpha_0 Z d_0^3 \left[1 - \exp\left(-\frac{\Delta\mu}{kT}\right)\right] \tag{8a}$$

for the so-called continuous or normal mode of growth (N) and

$$G_{2D} = S d_0 N_s D_{k2} \Gamma_2 \exp\left(-\frac{A_{k2}}{kT}\right) \tag{8b}$$

for growth rate moderated by two-dimensional (2-D) nucleation. In the above equations, D_{k3} and D_{k2} are the molecular fluxes connected with 3-D and 2-D nucleation, Γ_3 and Γ_2 are the so-called Zeldovich factors for 3-D and 2-D nucleation, A_{k3} and A_{k2} are the work of formation of 3-D and 2-D nuclei, $\Delta\mu$ is the thermodynamic driving force of the crystallization process, Z is the impingement rate of ambient phase molecules, α_0 is the relative number of growth sites, $N_1 \approx 1/d_0^3$ and $N_s \approx 1/d_0^2$ are the number of building units per unit volume of the surrounding phase and per unit surface of the growing crystal, d_0 and S being the average intermolecular spacing in the liquid and the surface of the 2-D nucleus, respectively. It is also assumed that $d_0 \approx d_k$, where d_k denotes the intermolecular spacing in the crystal.

The temperature dependences of A_{k3} and A_{k2} read

$$A_{k3} = \frac{16}{3}\pi \frac{\sigma^3 V_m^2}{\Delta\mu^2} \tag{9a}$$

and

$$A_{k2} = \pi \frac{\sigma^2 V_m d_0}{\Delta\mu} \tag{9b}$$

Here V_m is the molar volume of the crystallizing substance and σ is the specific surface energy at the liquid/crystal interface. For polymer crystals, two values of σ are defined: the lateral surface energy σ_s, corresponding to the crystalline faces formed by the stretched part of the chains, and the end surface energy σ_e, corresponding to the faces built by the polymer chain folds. However, as a first approximation, an effective value of $\bar{\sigma}^3 = \sigma_s^2 \sigma_e$ can be introduced [34, 35].

According to the empirical Turnbull–Scapski formula, an evaluation of $\bar{\sigma}$ can be given as

$$\bar{\sigma} = \gamma_0 \frac{\Delta S_m T_m}{N_a^{1/3} V_m^{2/3}} \tag{10}$$

Here ΔS_m is the entropy of melting, N_a is Avogadro's number and γ_0 is a numeric coefficient ranging from 0.3 to 0.6 for low molecular substances. In polymer nucleation and growth experiments, $\gamma_0 = 0.1$ and even lower values are found. An explanation of this finding is given below.

The temperature dependence of the thermodynamic driving force $\Delta\mu$ of the crystallization process in polymers can be given by Hoffman's approximation [16]

$$\Delta\mu = \int_0^T \Delta S(T)\mathrm{d}T \approx \Delta S_m \Delta T \frac{T}{T_m} \tag{11}$$

Here $\Delta T = T_m - T$ is the undercooling.

Considering Eqs. (3, 7–11), the temperature dependence of the rate coefficient K_s for an overall crystallization process involving sporadic nucleation and subsequent 2-D growth of clusters can be written as

$$K_s = \mathrm{const}_s \left(\frac{1}{\eta}\right)^n \exp\left(-\frac{A_{k3}}{kT}\left(1 + \frac{(n-1)A_{k2}}{A_{k3}}\right)\right)$$

$$\approx \mathrm{const}_s \left(\frac{1}{\eta}\right)^n \exp\left(-\frac{16}{3}\pi \frac{\sigma_s^2 \sigma_e V_m^2 T_m^2}{k\Delta S_m^2 \Delta T^2 T^3}\right) \tag{12a}$$

The temperature dependence of the rate coefficient K_a of 2-D growth of athermally existing spherulites is

$$K_a = \mathrm{const}_a \left(\frac{1}{\eta}\right)^{n-1} \exp\left(-\frac{(n-1)A_{k2}}{kT}\right)$$

$$= \mathrm{const}_a \left(\frac{1}{\eta}\right)^{n-1} \exp\left(-(n-1)\pi \frac{\sigma_s \sigma_e V_m d_0 T_m}{k\Delta S_m \Delta T T^2}\right) \tag{12b}$$

For $A_{k2}/A_{k3} \ll 1$ (see Eq.(9)), the right-hand side of Eq. (12a) follows immediately. It is seen that at low undercoolings, i.e. at $T \to T_m$, the rate coefficient in sporadic nucleation is totally determined by the steady state nucleation rate. In the same temperature region, K_a is determined by the growth rate.

According to the more general transient version of the theory of phase formation [12], the other basic parameter in nucleation, the non-steady-state time lag τ can be defined as

$$\tau = \frac{4}{3\pi\Gamma_3^2 D_{k3}} \tag{13a}$$

Taking into account the temperature dependence of D_{k3}, Eq. (13a) takes the form

$$\tau = \frac{\mathrm{const}}{\Delta\mu^2}\eta \tag{13b}$$

Here η is the bulk viscosity of the system.

When nucleation takes place in the presence of active substrates, i.e. crystallization cores, with activity Φ, we write [12,26]

$$I^* = N^* D^*_{k3} \Gamma^*_3 \exp\left(-\frac{A_{k3}\Phi}{kT}\right) \tag{14a}$$

$$\tau^* = \tau \Phi^{1/2} \tag{14b}$$

All quantities referring to heterogeneous nucleation are denoted here by *. The number of active crystallization sites in heterogeneous nucleation becomes $N^* = f^* N_1$, where f^* is a dimensionless coefficient.

4. Where to search for non-steady-state effects?

In analyzing the significance of non-steady-state effects, it has to be pointed out that when Eq. (5d) is applied, a linear dependence between the actually determined induction times τ_{ind}, the non-steady-state time lag τ, and the characteristic time $\tau_1 = (1/K_s)^{1/n}$, is to be expected, i.e.

$$\tau_{ind} = b\tau + \tau_1 = b\tau\left(1 + \frac{\tau_1}{b\tau}\right) \tag{15}$$

This approximation (introduced in Ref. [26]) gives a simple possibility for examining induction times and for determining the transient character of the nucleation process.

In considering the more complicated formalism given by Shi and Seinfeld (Eq. (5b)) or by Shneidman and Weinberg (Eq. (5c)), more complicated non-linear dependences between τ_{ind}, τ and τ_1 should be expected. In such cases, it becomes very difficult to predict the exact value of τ_{ind} and to assess the relative contribution of τ and τ_1 to τ_{ind}. Thus, the only way to determine the nature of the experimentally observed induction time remains to determine τ_{ind} in terms of Eq. (5d) and to analyze whether its temperature dependence is dominated by τ or by τ_1, which can only be done for cases where either $\tau_1 \gg \tau$ or $\tau \gg \tau_1$. In fact, this is the procedure adopted in the present contribution.

Taking into account Eq. (15) and the dependences derived in Section 3, it can easily be shown that for $n = 4$

$$\frac{\tau_1}{\tau} = \frac{\pi^3}{4}\left[\frac{5\times10^{-3}}{\gamma_0^{9/2}} \frac{(\Delta S_m/R)^{7/2} x^{9/2}(1-x)^8}{\left[1-\exp\left(-\frac{\Delta S_m}{R}(1-x)\right)\right]^3 \exp\left(-\frac{16}{3}\pi\gamma_0^3\left(\frac{\Delta S_m}{R}\right)\left(\frac{1}{x}\right)^3\left(\frac{1}{1-x}\right)^2\right)}\right]^{1/4} \tag{16a}$$

for normal growth and

$$\frac{\tau_1}{\tau}=\frac{\pi^3}{4}\left[\frac{5\times10^{-6}}{\gamma_0^{9/2}}\frac{(\Delta S_m/R)^2x^{9/2}(1-x)^{13/2}}{\exp\left(-\frac{16}{3}\pi\gamma_0^3\left(\frac{\Delta S_m}{R}\right)\left(\frac{1}{x}\right)^3\left(\frac{1}{1-x}\right)^2\left(1+\frac{9x(1-x)}{16\gamma_0}\right)\right)}\right]^{1/4} \tag{16b}$$

for 2-D growth.

When crystallization takes place in the presence of crystallization cores N^* with activity Φ, then

$$\frac{\tau_1^*}{\tau^*}=$$

$$\frac{\pi^3}{4\Phi^{1/2}}\left[\frac{5\times10^{-3}\Phi^{7/2}}{\gamma_0^{9/2}f^*}\frac{(\Delta S_m/R)^{7/2}x^{9/2}(1-x)^8}{\left[1-\exp\left(-\frac{\Delta S_m}{R}(1-x)\right)\right]^3}\frac{1}{\exp\left(-\frac{16}{3}\pi\gamma_0^3\Phi\left(\frac{\Delta S_m}{R}\right)\left(\frac{1}{x}\right)^3\left(\frac{1}{1-x}\right)^2\right)}\right]^{1/4} \tag{17a}$$

$$\frac{\tau_1^*}{\tau^*}=\frac{\pi^3}{4\Phi^{1/2}}\left[\frac{5\times10^{-6}\Phi^{7/2}}{\gamma_0^{9/2}f^*}\frac{(\Delta S_m{}^{/R})^2x^{9/2}(1-x)^{13/2}}{\exp\left(-\frac{16}{3}\pi\gamma_0^3\Phi\left(\frac{\Delta S_m}{R}\right)\left(\frac{1}{x}\right)^3\left(\frac{1}{1-x}\right)^2\left(1+\frac{9x(1-x)}{16\gamma_0\Phi}\right)\right)}\right]^{1/4} \tag{17b}$$

for normal and 2-D growth of crystals, respectively. In above equations, x denotes the reduced temperature, i.e. $x = T/T_m$.

Eqs. (16) are illustrated in Fig. 2 for different values of $\Delta S_m/R$ and γ_0. It should be noted that the absolute value of this ratio can be misleading, as far as there are a number of pre-exponential factors in Eqs. (7) and (8) expected according to nucleation theory, e.g. the Lothe Pound correction, etc., which can considerably change the magnitude of the above ratio. Nevertheless, the relative position of the curves in Fig. 2 implies some general trends:

(i) At $T/T_m \to 1$, the ratio τ_1/τ rises steeply. Here non-steady-state effects are never of any significance. This finding most probably explains the experimental results of previous authors, especially of Flory and McIntyre [15], that non-steady-state effects could not be found in the vicinity of the melting temperature T_m.

(ii) For growth determined by 2-D nucleation, steady state effects are more probable than for normal growth (see the relative position of curves 1 and 2 in Fig. 2a). However, it should be taken into account that when the values of $\Delta S_m/R$ approach unity (as for many inorganic glass-forming systems), the normal mechanism of growth becomes more probable (see Ref. [26] and references cited therein).

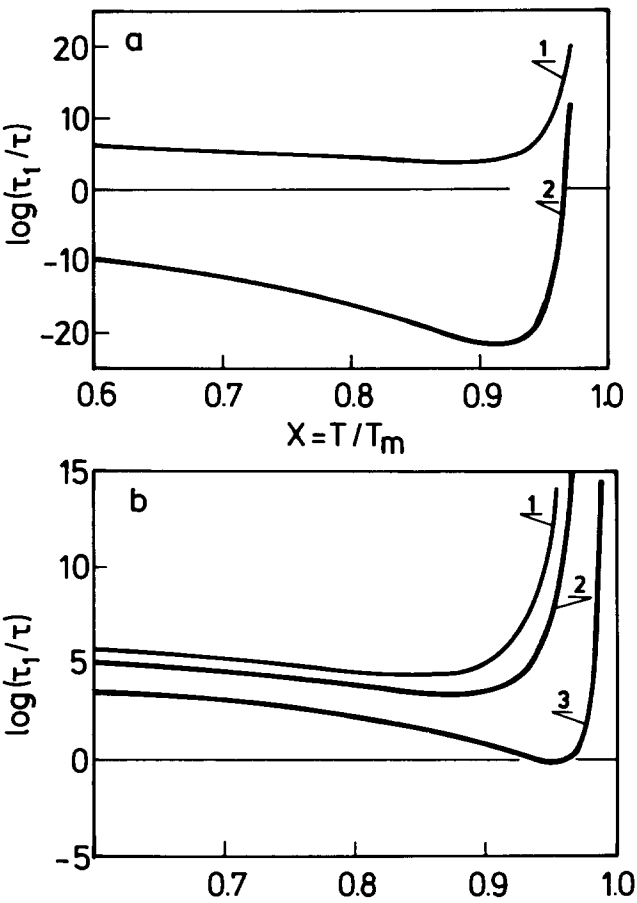

Fig. 2. Temperature dependence of the ratio τ_1/τ according to Eqs. (16). a. Influence of mode of growth: 1, normal growth; 2, growth determined by 2-D nucleation. In both cases $\gamma_0 = 0.1$ and $\Delta S_m/R = 3$. b. Influence of the thermodynamic parameter $\Delta S_m/R$ at normal growth: 1, $\Delta S_m/R = 3$; 2, $\Delta S_m/R = 2$; 3, $\Delta S_m/R = 1$. In all cases $\gamma_0 = 0.2$.

(iii) Heterogeneous nucleation dramatically alters the course of the τ_1/τ dependence (Eqs. (17)). It influences τ_1 exponentially while τ is changed only by $\Phi^{1/2}$ (see Eqs. (14)). Thus heterogeneous nucleation is a better possibility for demonstrating non-steady-state effects than the homogeneous case. That is why the first experimental proof for non-steady-state nucleation was given for a heterogeneous process (see Ref. [7]). In considering the particular case of polymer crystallization, it has to be taken into account that existing experimental data always give such low values of γ_0 that it should be assumed that even in the purest polymers there are active sites N^* and that here $N^* \rightarrow N_1$. In this sense, the activity Φ of any substrate in polymer nucleation should, in fact, only be considered as a relative quantity. The dependences on Fig. 3 are drawn with $\gamma_0 = 0.1$, assuming that very active nucleants are added.

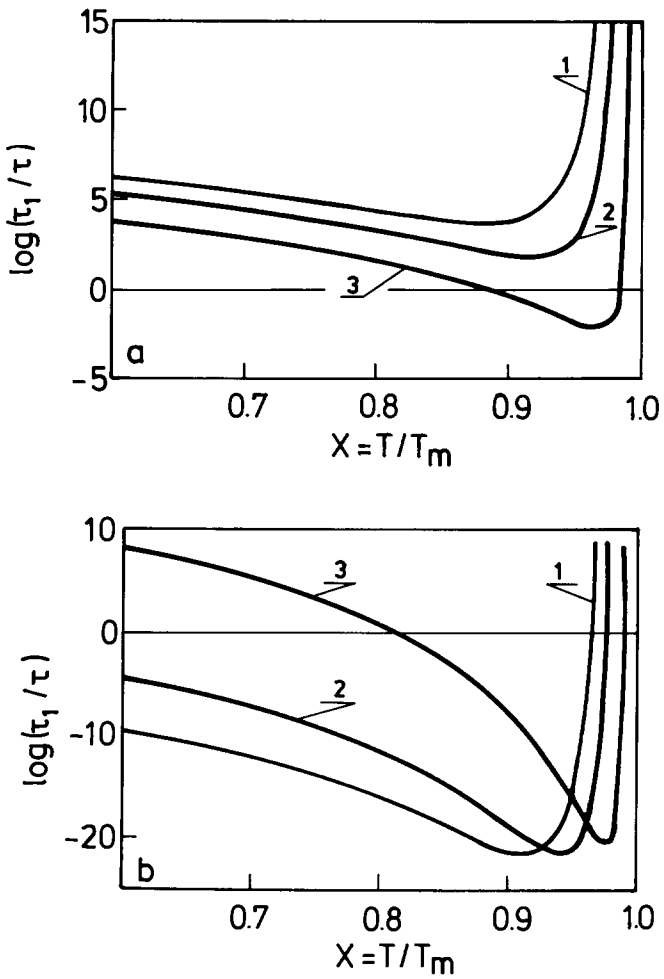

Fig. 3. Influence of the activity of substrates Φ on the temperature dependence of the ratio τ_1/τ according to Eqs. (17). a. Normal growth. b. Growth determined by 2-D nucleation: 1, $\Phi = 1$; 2, $\Phi = 0.5$; 3, $\Phi = 0.1$. In all cases $\gamma_0 = 0.1$, $\Delta S_m/R = 2$ and $f^* = 1 \times 10^{-2}$.

Overall, Figs. 2 and 3 indicate that polymer systems can be a very convenient model for demonstrating non-steady-state effects because of predominant 2-D growth mechanism and the expected low values of the product $\gamma_0\Phi$.

5. Experimental

Polyethylene terephthalate, without any fillers, having a molecular weight of 18400 corresponding to an average degree of polymerization $P = 95$, was specially synthesized for the purpose of the present investigation. The density of the amorphous polymer was $\rho = 1.35\,g\,cm^{-3}$. Fig. 4 gives a DSC trace of our material with a scan rate

of 5 K min^{-1}. It is seen from the figure that the glass transition temperature T_g of our samples is about 342 K. The melting temperature T_m of the materials used was determined as the temperature at which the last crystals melted. The measured value of T_m for our material was 542 K. The value of the enthalpy of melting ΔH_m of 100% crystalline PET was taken to be 135 J g^{-1} [36] which corresponds to an entropy of melting ΔS_m of our model polymer of 0.25 J g K^{-1}. In a previous study [16], it was found that the liquid/crystal difference of the specific heats $\Delta c_p(t)$ of PET is a constant in the temperature interval from T_m to T_g, and that $\Delta c_p(T)/\Delta S_m \approx 1.5$ (Fig. 5).

Fig. 6 shows the temperature dependence of the viscosity η as measured in Ref. [16]. In the vicinity of T_m, the viscosity was determined by Searle-type rotational viscometry. In the vicinity of T_g, data on the enthalpy relaxation of PET glass were used [39] to construct the $\eta(T)$ dependence, while at medium undercoolings ($T = 373$–383 K) the viscosity was assessed from the kinetics of relaxation of stress birefringence in thin vitrified PET samples. Details concerning the experimental procedure and the analysis of the results can be traced in our contribution cited above. It was found that the Vogel–Fulcher–Tammann equation satisfactorily describes the temperature dependence of η with $A = 10^{-1.4}$, $B = 1955$ and $T_\infty = 271$ K (see Fig. 6b). Fig. 6c gives the temperature dependence of the apparent activation energy of viscous flow of our PET samples.

TiO_2 particles (anatase) were used as crystallization-inducing agents. They were introduced into the polymer by a standard extrusion technique. The concentration of TiO_2 in our PET samples was 0.3%. The rheological study of our TiO_2-filled PET shows that Einstein's suspension formula describes the viscosity of the filled PET with an Einstein coefficient b_0 of 2.5. It was found that the activation energies for viscous flow for filled and unfilled samples are equal.

The crystallization of unfilled and TiO_2-seeded samples was investigated microscopically on polymer layers placed between two cover glasses in a hot stage. The polymer layer between the two cover glasses was fixed by heating for 10 min at 563 K and vitrifying the polymer by quenching the glass/polymer glass/glass "sandwich" in icy water. Our preliminary experiments showed that a heat treatment of 10 min at 563 K is sufficient to erase the crystallization memory of the polymer.

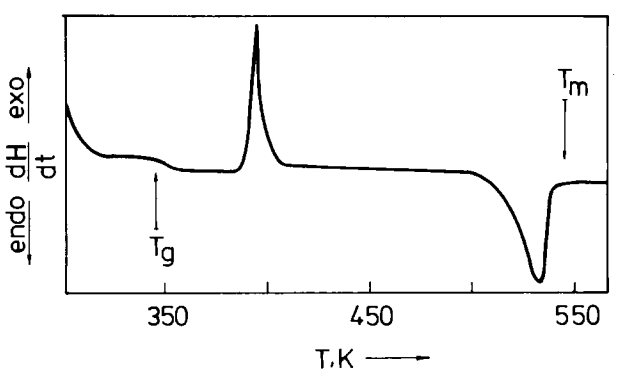

Fig. 4. Typical DSC trace of a vitrified PET sample heated with a scan rate of 5 K min^{-1}. Note the glass transition, the exothermic crystallization peak and the endothermic melting peak.

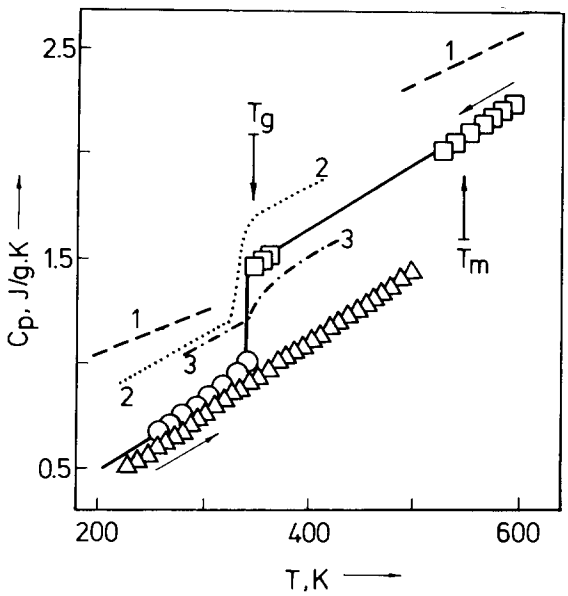

Fig. 5. Temperature dependence of the specific heats of PET according to data reported in the literature and to measurements performed in the present investigation: 1, data reported by Blundell et al. [36]; 2, data summarized and analyzed by Gaur et al. [37]; 3, data after Schick et al. [38]. The bold curve is drawn according to our results obtained in Ref. [16]: Δ, crystal; ○, glass; □, undercooled liquid.

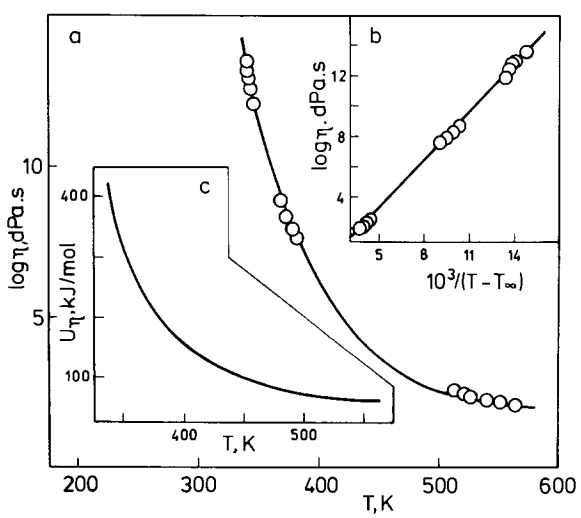

Fig. 6. Rheological behavior of PET: a, temperature dependence of the viscosity; b, Vogel–Fulcher–Tammann plot of the viscosity data; c, temperature dependence of the apparent activation energy of viscous flow $U\eta$. Data are taken from Dobreva [16].

Another type of sample containing athermal nucleation cores was prepared by preheating for only 4 min at a lower temperature (543 K) followed by quenching in icy water.

Crystallization measurements of unfilled and filled PET samples led to the determination of the time τ_{ind} necessary for the appearance of microscopically distinguishable

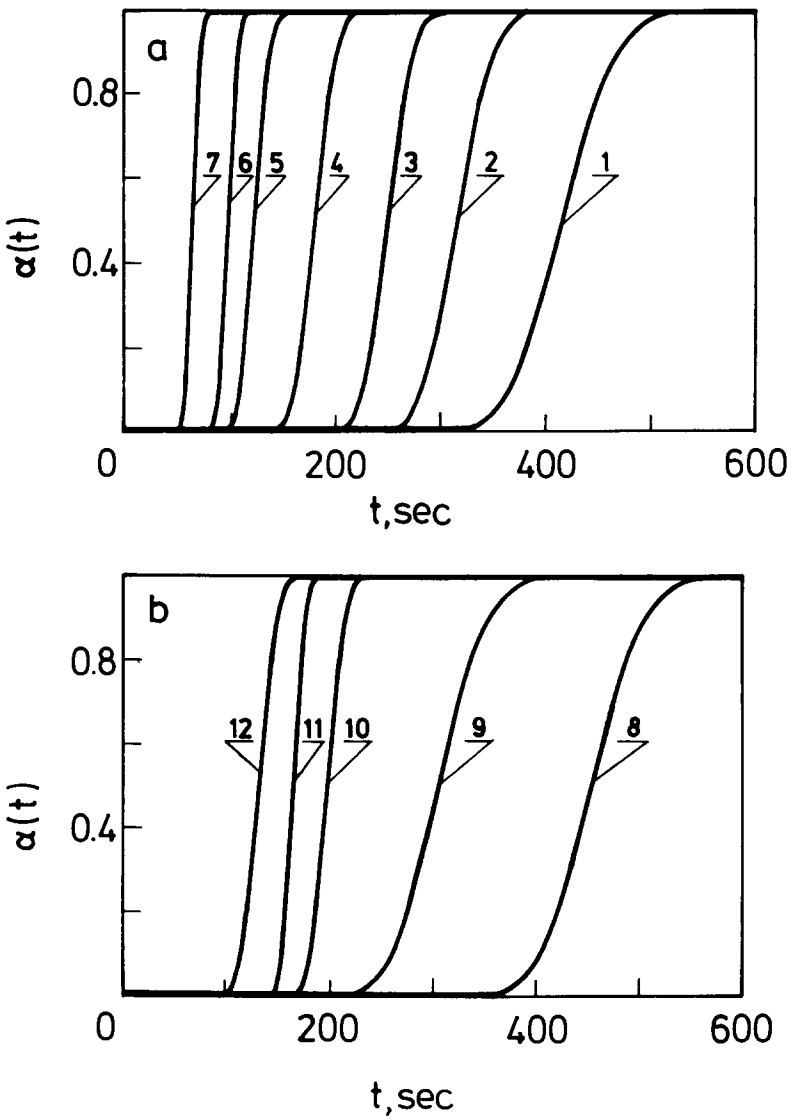

Fig. 7. Experimental $\alpha(t)$ curves for unfilled PET (a) and for PET containing TiO_2 (b) crystallized sporadically at high undercoolings. a. 1, 367 K; 2, 369 K; 3, 371 K; 4, 373 K; 5, 375 K; 6, 377 K; 7, 379 K. b. 8, 363 K; 9, 365 K; 10, 367 K; 11, 369 K; 12, 371 K. Note that at the same temperature, curves for PET containing TiO_2 are shifted to lower times (compare curves 1, 2, 3 from (a) with curves 10, 11, 12 from (b)).

crystallization at constant temperature. The apparatus time τ_a for the PET samples to reach the crystallization temperature was determined by special experiments. It was shown that τ_a is negligible as compared with the induction times determined in the present investigation.

In order to study the course of the overall crystallization kinetics, a Mettler differential scanning calorimeter coupled with a microprocessor was used. Calibration of the instrument was done using standard procedures. Measurements from the molten state in the vicinity of T_m, as well as from the glassy state in the vicinity of T_g, were performed. Two types of samples were used:

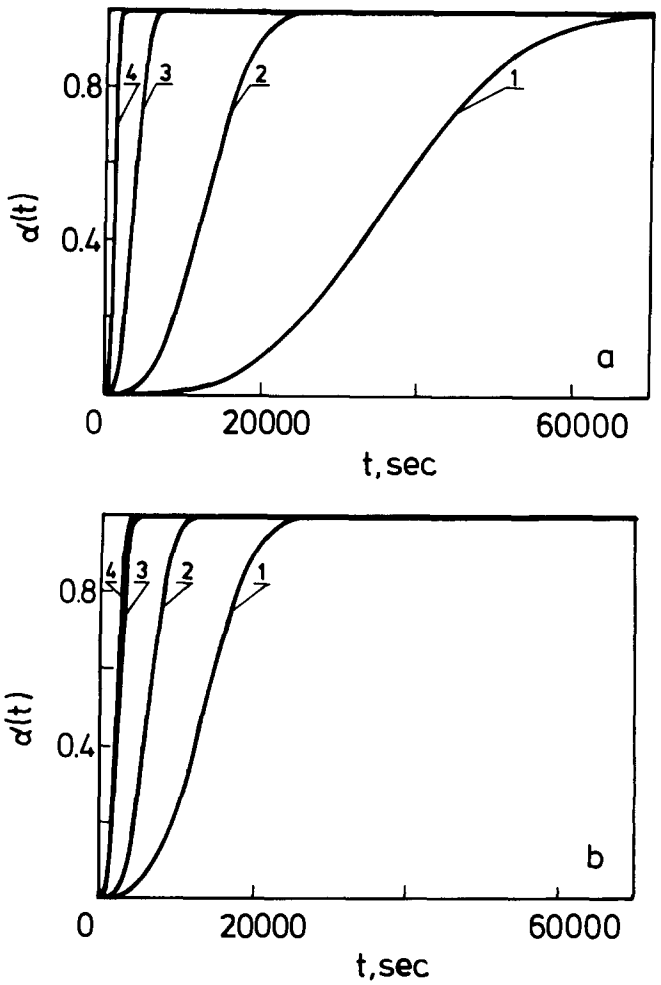

Fig. 8. Experimental $\alpha(t)$ curves for unfilled PET (a) and for PET containing TiO_2 (b) crystallized sporadically at low undercoolings: 1, 518 K; 2, 519 K; 3, 521 K; 4, 522 K.

(i) samples in which sporadic nucleation took place, i.e. samples heated at 563 K for 10 min; and

(ii) samples containing athermal nuclei, i.e. samples heated at 543 K for 4 min. Vitreous PET was obtained by quenching in icy water.

Each experimental determination (including calorimetry and optical microscopy) was repeated at least three times and the average value was taken as a representative one.

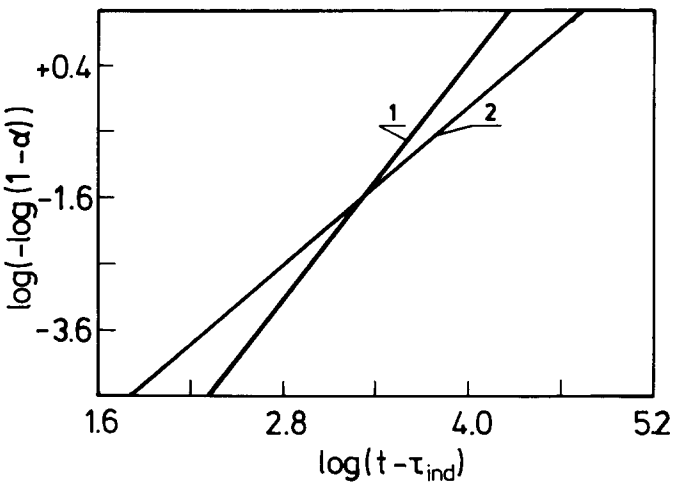

Fig. 9. Log(−log(1 − α)) vs. log ($t - \tau_{ind}$) dependence in terms of Eq. (18) for PET crystallized at 373 K: 1, sporadic nucleation with $\tau_{ind} = 139$ s; 2, athermally nucleated samples with $\tau_{ind} \approx 0$.

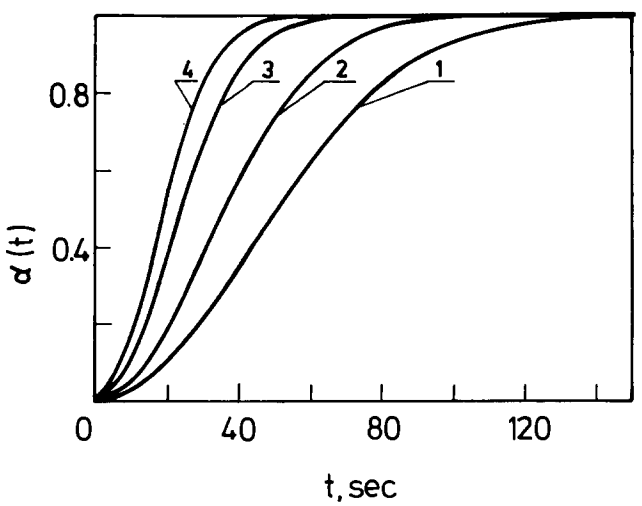

Fig. 10. Experimental α(t) curves for PET samples containing athermal nuclei crystallized at high undercoolings: 1, 373 K; 2, 375 K; 3, 377 K; 4, 379 K.

A computer program for linear and non-linear regression analysis was used to process the experimentally obtained crystallization dependences (the DSC $\alpha(t)$ curves). Using a linear fitting procedure, the computer analysis gave the induction time τ_{ind}, the rate coefficient K, and the Avrami exponent n, for each temperature assuming that in accordance with Eqs. (5) and (5d) we can write

$$a \approx \begin{cases} 0 & 0 \leqslant t \leqslant \tau_{ind} \\ 1 - \exp[-Kt^n(1 - \tau_{ind}/t)^n] & \tau_{ind} < t < \infty \end{cases} \tag{18}$$

A non-linear regression procedure was used to assess the kinetic parameters in Eqs. (5) and (5a) (K, n, τ), in Eqs. (5) and (5b) (K, n, τ, τ_e) and in Eqs. (5) and (5c) ($K, n, \tau, A_{k3}/kT$). Several sets of parameters describing each experimental DSC $\alpha(t)$ curve were found, without it being possible to attach any reasonable physical meaning to any of them. This is why we considered only the results obtained by the double-logarithmic fitting procedure according to Eq. (18). The temperature dependences of the values of the induction times thus obtained and the kinetic rate coefficients were examined in order to determine the dominant contribution of τ or τ_1 to τ_{ind}.

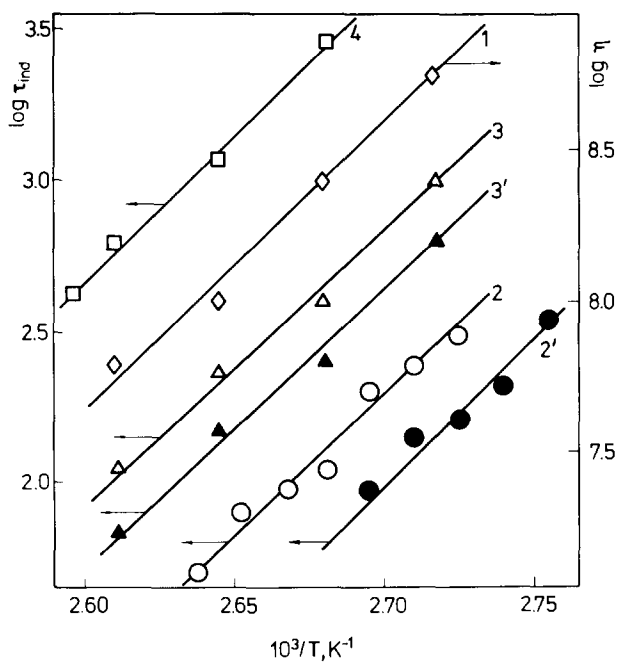

Fig. 11. Temperature dependence of τ_{ind} in sporadic crystallization regime in the vicinity of T_g: 1, temperature dependence of the viscosity η; 2, 2', temperature dependence of τ_{ind} determined from the analysis of the DSC $\alpha(t)$ curves for unfilled PET and for PET containing TiO_2, respectively; 3, 3', temperature dependence of the induction times for the onset of crystallization determined by optical microscopy for unfilled PET and for PET containing TiO_2, respectively; 4, temperature dependence of τ_{ind} according to microscopic determinations reported in Ref. [35]. Note that the apparent activation energies are equal in all cases.

6. Experimental results and discussion

Figs. 7 and 8 give a number of experimental $\alpha(t)$ curves for unfilled and filled PET at low and at high undercoolings, respectively. It is seen that TiO_2 particles reduce the induction time for the onset of crystallization in both crystallization above the glassy state and in crystallization from the undercooled liquid. It has to be pointed out that in determining the overall isothermal crystallization kinetics by DSC experiments, the time registration begins after the elapse of the apparatus time τ_a, which again is $\tau_a \ll \tau_{ind}$.

Fig. 9 shows the $\log(-\log(1-\alpha))$ vs. $\log(t-\tau_{ind})$ plot for a given temperature for unfilled PET crystallized under sporadic and athermal regimes, respectively, according to Eq. (18). It should be mentioned that for PET samples with athermal nucleation the slope of the considered dependence is always lowered by unity when compared with the sporadic nucleation case.

Fig. 10 shows the $\alpha(t)$ curves for unfilled PET containing athermal nuclei, i.e. heat treated at 543 K for 4 min. The overall crystallization behavior of PET containing TiO_2 results in analogous curves. The values for the induction times for unfilled and filled samples differ only within the limits of the experimental error. The values of n for both unfilled and TiO_2-initiated athermally crystallized samples are equal to 2, while for the sporadic nucleation case in both unfilled and TiO_2-nucleated samples, $n \approx 3$. This implies that in terms of the Avrami analysis in samples heat treated at 543 K for 4 min,

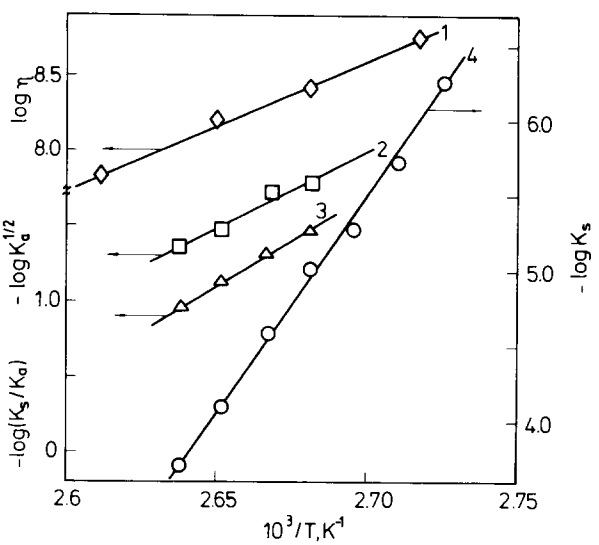

Fig. 12. Temperature dependence of the rate coefficients in sporadic K_s and athermal K_a crystallization regimes at high undercoolings in the vicinity of T_g: 1, temperature dependence of the viscosity η; 2, temperature dependence of K_a; 3, temperature dependence of the ratio K_s/K_a; 4, temperature dependence of K_s. See text for the values of the respective activation energies calculated from the slopes of these dependences.

the crystallization process is athermally predetermined, i.e. only growth of the already existing spherulites is observed.

Fig. 11 shows the temperature dependence of the induction times for the onset of crystallization in the vicinity of T_g as determined by our procedure. The temperature dependence of the viscosity in the same temperature region is also depicted in the figure. It is seen that the slope of the $\log \tau_{ind}$ vs. $1/T$ dependence is approximately equal to the $\log \eta$ vs. $1/T$ slope, and amounts to 40 kcal mol^{-1} in accordance with the analysis in Section 4 (see Eqs. (13b) and (15)). This means that the induction time for the onset of crystallization at $T \rightarrow T_g$ is entirely dominated by the non-steady-state time lag. The induction times determined microscopically are greater than the corresponding induction times obtained by calorimetric measurements but nevertheless the same slope is observed. The higher values of τ_{ind} determined microscopically may be due to the fact that the nuclei formed have to grow to visible sizes in order to be detected.

The shift of the $\log \tau_{ind}$ vs. $1/T$ dependence for the filled polymer from the corresponding dependence for the unfilled polymer allows calculation of the activity of

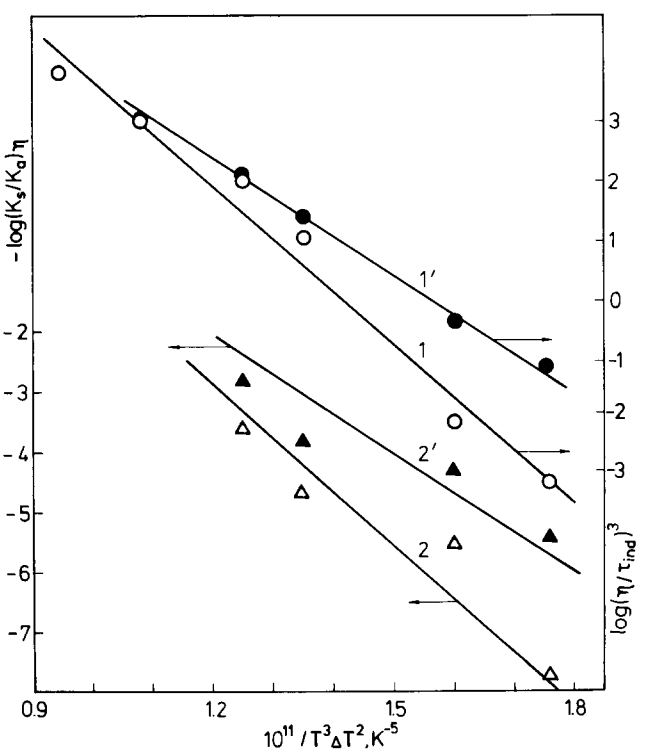

Fig. 13. Temperature dependence of the induction times and the rate coefficients for PET samples crystallized at low undercoolings in the vicinity of T_m: 1, $\log(\eta/\tau_{ind})^3$ vs. $1/T^3\Delta T^2$ dependence for PET; 1′, $\log(\eta/\tau_{ind})^3$ vs. $1/T^3\Delta T^2$ dependence for PET containing TiO_2; 2, $\log(K_s/K_a)_\eta$ vs. $1/T^3\Delta T^2$ dependence for PET in terms of Eqs. (12); 3, $\log(K_s/K_a)_\eta$ vs. $1/T^3\Delta T^2$ dependence for PET containing TiO_2 in terms of Eq. (12).

TiO_2 particles according to Eq. (14b) for both microscopic and calorimetric determinations. The value of Φ is approximately 0.8.

In considering Fig. 11, it is seen that our previous experimental data for τ_{ind} in the vicinity of T_g [35] also yield the same slope of the log τ_{ind} vs. $1/T$ dependence. For polymers, the activation energy for viscous flow is usually independent of the molecular weight. Therefore, induction times obtained in PET in different samples and by different authors can be compared.

Fig. 12 shows the temperature dependence of the rate coefficients K_s and K_a and their ratio for devitrification experiments. The temperature dependence of the viscosity is given again. From the log $K_a^{1/2}$ vs. $1/T$ plot, the activation energy for crystal growth according to Eq. (3b) is calculated as approximately 45 kcal mol^{-1}. Taking into account that the activation energy for viscous flow U_η is about 40 kcal mol^{-1}, it turns out that the work of 2-D nucleation is about 5 kcal mol^{-1}, which is a very reasonable value.

The slope of the log K_s/K_a vs. $1/T$ dependence (curve 3) gives an activation energy for homogeneous nucleation of 60 kcal mol^{-1}. The work of three-dimensional nucleation can be estimated to be about 11 kcal mol^{-1}.

Finally, Fig. 12 gives the log K_s vs. $1/T$ dependence (curve 4) for the sporadic overall crystallization process, the slope of which is about 140 kcal mol^{-1}. This is a reasonable value taking into account Eq. (3a) and the values of U_η, A_{k2} and A_{k3}.

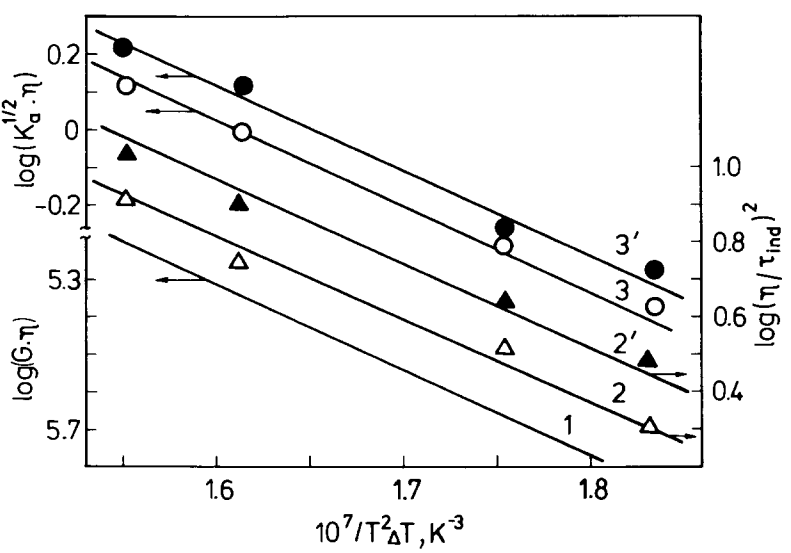

Fig. 14. Temperatrure dependence of the kinetic parameters in overall athermal crystallization in PET samples at low undercoolings in the vicinity of T_m: 1, temperature dependence of the linear growth rate in PET from Ref. [20]; 2, 2',-temperature dependence of τ_{ind} for PET and PET containing TiO_2; respectively; 3, 3', temperature dependence of K_a for PET and PET containing TiO_2, respectively. Note that the apparent activation energies in all cases are equal and that the induction times in the athermal crystallization regime at low undercoolings are determined by the growth of crystallites to detectable sizes.

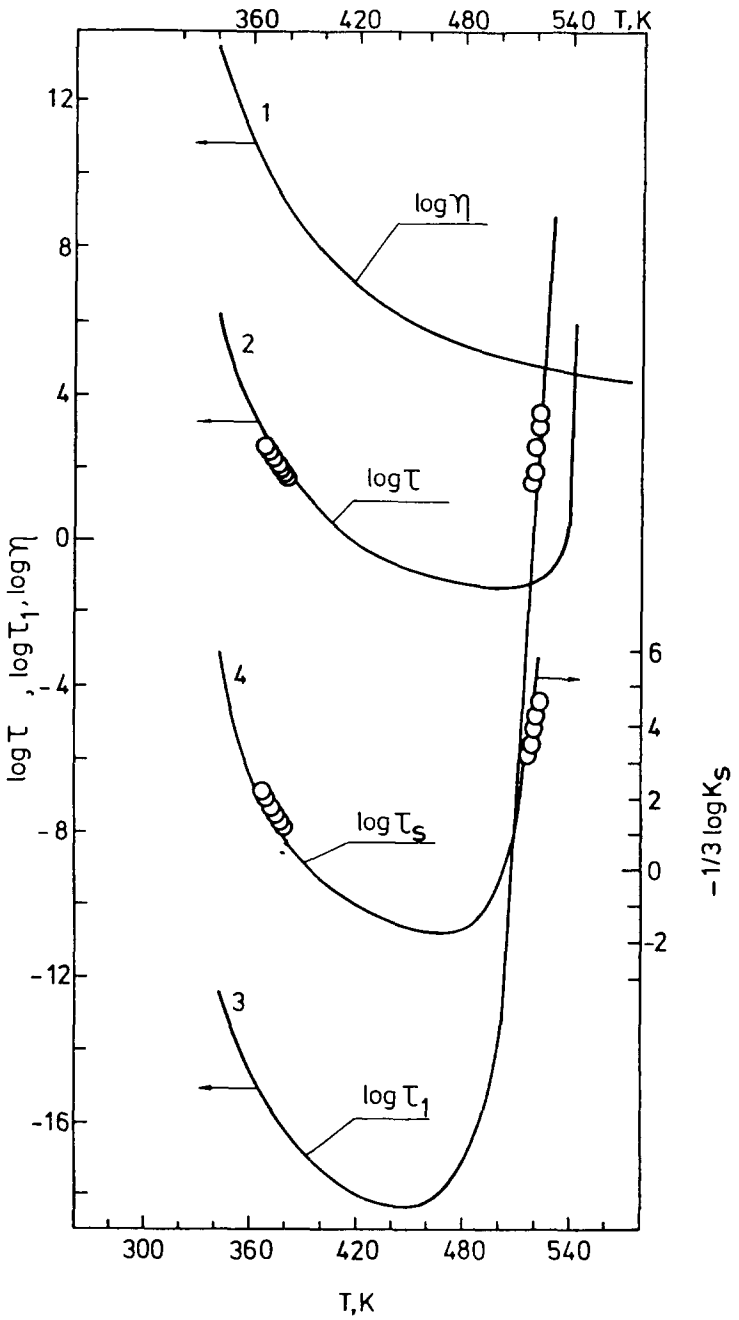

Fig. 15. Temperature dependence of the viscosity, non-steady-state time lag, steady-state nucleation rate and sporadic crystallization rate coefficient: 1, temperature dependence of the viscosity η; 2, temperature dependence of the non-steady-state time lag τ calculated according to Eq. (13b); 3, temperature dependence of the steady-state nucleation rate, $\tau_1 = 1/I_0$, calculated according to Eq. (7); 4, temperature dependence of the sporadic crystallization rate coefficient $\tau_s = (1/K_s)^{1/3}$ calculated according to Eqs. (3a) and (12a). The respective experimental data, determined according to our procedure in terms of Eq. (18) from the analysis of the DSC $\alpha(t)$ curves, are shown (○). The curves are drawn with experimentally determined constants.

The temperature dependences of the kinetic parameters of the crystallization process taking place at low undercoolings under sporadic conditions are presented in Fig. 13. The slope of the $\log(\eta/\tau_{ind})^3$ vs. $1/T^3\Delta T^2$ dependence is equal to the slope of the $-\log(K_s/K_a)\eta$ vs. $1/T^3\Delta T^2$ dependence, which implies that the induction time for the onset of crystallization under sporadic conditions at low undercoolings is determined by the steady-state nucleation rate (see Eq. (12)). It is calculated that the product $\sigma_s^2\sigma_e$ amounts to 372 erg^3 cm^{-6}. From the ratio of the slopes of the $\log(\eta/\tau_{ind})^3$ vs. $1/T^3\Delta T^2$ dependences for the homogeneous and heterogeneous case, the value of Φ is assessed to be 0.8.

Fig. 14 gives the results from athermal crystallization experiments at low undercoolings. The temperature dependence of the growth rate G as reported by van Antwerpen and van Krevelen [20] is also illustrated. It is seen from the figure that the $\log(\eta/\tau_{ind})^2$ and $\log(K_a^{1/2}\eta)$ dependences have the same slopes for the homogeneous and heterogeneous cases. From the slope of the straight lines, the product $\sigma_s\sigma_e$ is calculated to be 98 erg^2 cm^{-4}. From the ratio of the products $\sigma_s^2\sigma_e$ and $\sigma_s\sigma_e$ found for sporadic and athermal crystallization experiments, it follows that $\sigma_e = 26$ erg cm^{-2} and $\sigma_s = 4$ erg cm^{-2}. It has to be mentioned, however, that the above procedure would be correct only in the case of real homogeneous nucleation, i.e. if $\Phi = 1$. Because comprehensive data for the temperature dependence of the nucleation rate in PET are lacking, this assumption cannot be confirmed experimentally.

7. Conclusions

The thorough analysis described shows that it is very difficult or even practically impossible to distinguish between the various theoretical concepts (Eqs. (5)) used in describing non-steady-state kinetics of overall crystallization from experimental $\alpha(t)$ curves obtained by DSC measurements. That is why the simplest possible assumption is adopted in the present contribution, i.e. that non-steady-state effects lead to (or at least can be approximately described by) a linear shift along the time axis. This assumption makes it possible to determine the kinetic parameters of the overall crystallization process by using a standard linear regression procedure. A subsequent analysis of the temperature dependence of the induction times thus found can determine whether or not non-steady-state effects are involved.

The analysis of the experimental data, performed in the previous section, shows that in fact from a physical point of view not every induction time τ_{ind} is a non-steady-state time lag. On the contrary, as shown in Fig. 15, non-steady-state effects surpass the time necessary for detectable crystallization only in the vicinity of the glass transition temperature T_g. A temperature range follows where the values of both τ and τ_1 are in balance. However, at $T \rightarrow T_m$, the values of τ_1 are considerably higher than τ and the induction time is determined only by τ_1.

Experimental evidence for the existence of non-steady-state induction times in the kinetics of crystallization of PET in the vicinity of the glass transition temperature, provided by Imai et al. [40], is worth mentioning. These authors have found that near T_g for periods lower than the value of τ_{ind} determined by us, a population of

submicroscopical crystalline clusters can be detected by small-angle X-ray scattering. In our opinion, this experimental finding gives direct proof for the transient nature of nucleation in polymers.

In conclusion, we would like to point out that with the present investigation non-steady-state effects have been found for the three structural classes of glass-forming liquids: inorganic oxide systems including inorganic polymers, metal glass-forming alloys, and organic chain-folding polymers. Thus, non-steady-state effects are inherent to the very nature of the nucleation process.

References

[1] J.B. Zeldovich, Acta Physchim. USSR, 18 (1943) 1.
[2] J. Feder, K.C. Russel, J. Lothe and G.M. Pound, Adv. Phys., 15 (1966) 111.
[3] B.Ya. Lyubov and L.A. Roitburd, in Problems of Metallography and Metal Physics (Russ.), Metalurgizdat, Moscow, 1958, Vol. 5, p. 91.
[4] F.G. Collins, Z. Electrochem., 59 (1955) 404.
[5] D. Kashchiev, Surf. Sci., 14 (1969) 209.
[6] F.K. Kelton, A.L. Greer and G.V. Thompson, J. Phys. Chem., 79 (1983) 6261.
[7] I. Gutzow, S. Toschev, M. Marinov and E. Popov, Krist. Techn., 3 (1968) 37.
[8] I. Gutzow and S. Toschev, in Advances in L.L. Hench and S.W. Freiman (Eds.), Nucleation and Crystallization of Glasses, Am. Ceram. Soc., Columbus OH, 1971, p. 10.
[9] P.F. James, Phys. Chem. Glasses, 15 (1974) 122.
[10] A. Kalinina, B.M. Fokin and V.A. Philipovich, Phys. Chem. Glasses (Russ.), 3 (1977) 122.
[11] S. Toschev and I. Gutzow, Phys. Status Solidi, 21 (1967) 683.
[12] I. Gutzow, Contemp. Phys., 21 (1980) 121, 243.
[13] F.K. Kelton, in H. Ehrenheich and D. Turnbull (Eds.), Solid State Physics, Academic Press Inc., Boston, 1991, Vol. 45, p. 75.
[14] S. Budurov, T. Spasov, V. Dyakovich, G. Konezos and A. Lovas, Int. Conf. Rapidly Quenched Met. Alloys, 1988, p. 85.
[15] P.J. Flory and A.D. McIntyre, J. Polym. Sci., 8 (1955) 592.
[16] A. Dobreva, Ph.D. Thesis, Sofia, 1992.
[17] A. Sharples, Polymer, 3 (1962) 250.
[18] A. Sharples and F.L. Swinton, Polymer, 4 (1963) 119.
[19] V.G. Baranov, A.V. Kenarov and T.I. Volkov, J. Polym. Sci., C30 (1970) 271.
[20] F. van Antwerpen and D.W. van Krevelen, J. Polym. Sci. Phys., 10 (1972) 2423.
[21] H.J. Kolb and E.F. Izard, J. Appl. Phys., 20 (1949) 564.
[22] A. Keller, G.R. Lester and L.B. Morgan, Philos. Trans. R. Soc. London Ser. A, Math. Phys. Sci., 921 (1954) 1.
[23] F. Rybnikar, Coll. Czech. Chem. Commun., 25 (1960) 1529.
[24] W.H. Cobbs and R.L. Burton, J. Polym. Sci., 10 (1953) 275.
[25] I. Gutzow and D. Kashchiev, in L.L. Hench and S.W. Freiman (Eds.), Advances in Nucleation and Crystallization of Glasses, Am. Ceram. Soc., Columbus OH, 1971, p. 116.
[26] I. Gutzow, D. Kashchiev and I. Avramov, J. Non-Cryst. Solids, 74 (1985) 477.
[27] A.N. Kolmogorov, Bull. Acad. Sci. USSR (Sci. Mater. Nat.), 3 (1937) 355.
[28] W.A. Johnson and R.F. Mehl, Trans. AIME, 135 (1939) 416.
[29] M. Avrami, J. Chem. Phys., 7 (1939) 1103; 8 (1940) 21; 9 (1941) 177.
[30] K. Mampel, Z. Phys. Chem., A187 (1940) 43, 225.
[31] O.M. Todes, Zh. Phys. Chim. USSR, 14 (1940) 1224.
[32] V.A. Schneidman and M.C. Weinberg, J. Non-Cryst. Solids, 160 (1993) 89.
[33] G. Shi and J.H. Seinfeld, J. Mater. Res., 6 (1991) 2091, 2097.

[34] L. Mandelkern, Crystallization of Polymers, McGraw-Hill, New York, 1964.
[35] I. Gutzow, V. Dochev, E. Pancheva and K. Dimov, J. Polym. Sci. Polym. Phys., 16 (1978) 1156.
[36] D.J. Blundell, D.R. Beckett and P.H. Willcocks, Polymer, 22 (1981) 707.
[37] U. Gaur, S. Lau, B.B. Wunderlich and B.J. Wunderlich, Phys. Chem. Ref. Data, 12 (1983) 65.
[38] C. Schick, L. Kramer and W. Mischok, Acta Polym., 36 (1985) 47.
[39] I. Avramov, N. Avramova and S. Fakirov, J. Polym. Sci. Polym. Phys., 27 (1987) 2419.
[40] M. Imai, K. Mori, T. Mizukami, K. Kaji and T. Kanaga, Polymer, 33 (1992) 4451, 4457.